PFKFB4 control of AKT signaling is essential for premigratory and migratory neural crest formation

Ana Leonor Figueiredo[1,2], Frédérique Maczkowiak[1,2], Caroline Borday[1,2], Patrick Pla[1,2], Meghane Sittewelle[1,2], Caterina Pegoraro[1,2] and Anne H. Monsoro-Burq[1,2,3,*]

ABSTRACT

Neural crest (NC) specification comprises an early phase, initiating immature NC progenitors formation at neural plate stage, and a later phase at neural fold stage, resulting in a functional premigratory NC that is able to delaminate and migrate. We found that the NC gene regulatory network triggers upregulation of *pfkfb4* (6-phosphofructo-2-kinase/fructose-2,6-bisphosphatase 4) during this late specification phase. As shown in previous studies, PFKFB4 controls AKT signaling in gastrulas and glycolysis rate in adult cells. Here, we focus on PFKFB4 function in NC during and after neurulation, using time-controlled or hypomorph depletions *in vivo*. We find that PFKFB4 is essential both for specification of functional premigratory NC and for its migration. PFKFB4-depleted embryos fail to activate *n-cadherin* and late NC specifiers, and exhibit severe migration defects resulting in craniofacial defects. AKT signaling mediates PFKFB4 function in NC late specification, whereas both AKT signaling and glycolysis regulate migration. These findings highlight novel and essential roles of PFKFB4 activity in later stages of NC development that are wired into the NC gene regulatory network.

KEY WORDS: Neural crest, *Xenopus laevis* embryo, PFKFB, 6-Phosphofructo-2-kinase/fructose-2, 6-bisphosphatase, AKT, Migration, Glycolysis, Neural plate border

INTRODUCTION

The neural crest (NC), a migratory and multipotent cell population in vertebrate embryos, forms many differentiated cell types, including pigment cells, craniofacial skeleton, peripheral neurons and glia (Bronner and Le Douarin, 2012). NC development starts during gastrulation, at the edges of the neural plate, and continues until late organogenesis. In early gastrulas, signals from the adjacent neural plate, non-neural ectoderm, and underlying mesoderm specify the neural border (NB), a transition area located across the neural plate and the non-neural ectoderm (Saint-Jeannet et al., 1997; Wilson et al., 1997; Neave et al., 1997, Chang and Hemmati-Brivanlou, 1998; LaBonne and Bronner-Fraser, 1998; Villanueva et al., 2002; Monsoro-Burq et al., 2003, 2005; Milet and Monsoro-Burq, 2012; Meulemans and Bronner-Fraser, 2004; Basch et al., 2006). The NB is a mixed territory comprising prospective dorsal neural tube cells, NC and cranial placode progenitors (Steventon et al., 2009; Pegoraro and Monsoro-Burq, 2012).

In late gastrulas and early neurulas (neural plate stage), NC specification begins within the NB, upon the coordinated action of WNT signaling and the broad activation in this region of several transcription factors [PAX3/7, ZIC1/2, MSX1/2, TFAP2A, GBX2, HES4, AXUD (CSRNP1), cMYB (MYB); Luo et al., 2003; Brewer et al., 2004; Monsoro-Burq et al., 2005; Sato et al., 2005; Khadka et al., 2006; Basch et al., 2006; Nichane et al., 2008; Li et al., 2009; Maczkowiak et al., 2010; de Crozé et al., 2011; Simões-Costa et al., 2015]. This initial phase of NC specification is marked by locally enhanced expression of *tfap2a* and *hes4*, and low-level *snail2* (*snai2*) and *foxd3*, two transcription factors marking early NC progenitors, i.e. lineage-restricted cells that are still functionally immature (Saint-Jeannet et al., 1989; Essex et al., 1993; Nieto et al., 1994; Mayor et al., 1995; Mancilla and Mayor, 1996; Nichane et al., 2008; de Crozé et al., 2011). During the second half of neurulation, as neural folds elevate, the immature NC is further specified into functional premigratory NC, ready to undergo epithelium-to-mesenchyme transition (EMT) and migration. The fully specified NC (mature) is characterized by the late markers *sox10*, *twist1*, *tfap2e*, enhanced *ets1* and *cmyc* (Bellmeyer et al., 2003; Théveneau et al., 2007). In late neurulas, after EMT, NC cells migrate along defined embryonic routes, maintaining *sox10* and *twist1* expression (Theveneau and Mayor, 2012). Importantly, TWIST1 is essential for the coordinated action of EMT regulators SNAIL1/2 (Lander et al., 2013), and NC acquires enhanced survival properties (Vega et al., 2004). Finally, the cranial NC populates the craniofacial prominences and differentiates into mesenchyme, cartilage and bone (Le Douarin and Kalcheim, 1999).

We found that *pfkfb4* (*6-phosphofructo-2-kinase/fructose-2,6-bisphosphatase*) expression was upregulated during late NC specification/maturation phase (neural fold stage). In adult cells, PFKFB1-4 control the cytoplasmic levels of fructose-2,6-bisphosphate, the strongest allosteric activator of phosphofructokinase1, the enzyme catalyzing the rate-limiting reaction of glycolysis (Okar et al., 2001; Pilkis et al., 1995, Fig. S1). By its strong kinase activity, PFKFB4 promotes glycolysis in adults (Okar et al., 2001) and in neurula-stage embryos (this study). Moreover, in embryos, we have previously shown that PFKFB4 is essential for global ectoderm regionalization, by glycolysis-independent control of AKT signaling (Pegoraro et al., 2015). Here, we found that the NC gene regulatory network (NC-GRN) triggers elevated *pfkfb4* expression during premigratory NC maturation. Using either constitutive or time-controlled PFKFB4 depletions, and time-controlled pharmacological inhibition of PI3K-AKT signaling *in vivo*, we show that PFKFB4 and AKT signaling regulate a timely switch between lineage-restricted but immature NC and functional premigratory NC. Furthermore, after EMT, PFKFB4 controls NC migration through both PI3K-AKT signaling and glycolysis. These

[1]UMR 3347-U1021, Univ. Paris Sud, Université Paris Saclay, CNRS, INSERM, Centre Universitaire, 15, rue Georges Clémenceau, F-91405, Orsay, France. [2]UMR 3347-U1021, Institut Curie Research Division, PSL Research University, F-91405, Orsay, France. [3]Institut Universitaire de France, MENRT, 75005 Paris cedex 05, France.

*Author for correspondence (anne-helene.monsoro-burq@curie.fr)

A.L.F., 0000-0003-2329-2854; C.P., 0000-0002-8935-8978; A.H.M.-B., 0000-0003-2427-982X

DEVELOPMENT

results suggest that NC developmental progression relies upon continuous function of PFKFB4, as a novel NC-GRN actor, activity of which is relayed by AKT signaling.

RESULTS

Pfkfb4 expression labels the NC during second half of neurulation

NB induction starts in early *Xenopus laevis* gastrulas [stage (st.) 10.5; Nieuwkoop and Faber, 1994], characterized by expression of *pax3*, *zic1/2* and *hes4* lateral to the neural plate (de Crozé et al., 2011; Nichane et al., 2008). NC specification starts at the end of gastrulation (st.11.5-12), marked by the early NC specifiers *snail2* and *foxd3* at neural plate stage (st.12-14; Fig. 1A). NC specification is further established (maturation) during neural fold stage (st.14-18), with activation of late NC specifiers and EMT inducers (*sox10*, *twist1*), and increased expression of early NC specifiers (Fig. 1B). Upon neural tube closure (st.17-19), cranial NC cells undergo EMT and migrate towards the branchial arches and craniofacial areas around tailbud st.24 (Fig. 1C).

We previously found that *pfkfb4* is enriched in premigratory NC (Plouhinec et al., 2014). At neural plate stage, *pfkfb4* was expressed at low levels throughout the dorsal ectoderm (Fig. 1D). At early neural fold stage (st.14), later than *snail2* initiation, *pfkfb4* was strongly enriched in the NB/NC (Fig. 1E,F,L-N). At the end of neurulation (st.18), NC *pfkfb4* mRNA levels, but not *pfkfb1-3* levels, were elevated by 1.5-fold compared with whole embryo expression (Fig. 1J, Fig. S2). The premigratory NC expressed 6.4-fold higher *pfkfb4* levels than the adjacent anterior neural fold (future forebrain and placodes). *pfkfb4* was expressed during NC EMT and early migration but decreased as NC cells reached craniofacial areas (Fig. 1H,I). This pattern contrasted with blastula and gastrula stages, when low *pfkfb4* levels were detected in the entire dorsal ectoderm, encompassing the neural plate, the NB and part of the non-neural ectoderm (Pegoraro et al., 2015). Thus, *pfkfb4* was enriched in premigratory NC, as well as during its maturation period, NC EMT and early migration (st14-22).

PFKFB4 activation promotes NC formation at the neural border

Experimental increase of PFKFB4 levels *in vivo* led to a moderate but reproducible increase of NB and early NC marker expression at neural plate stage (st.14; *pax3, zic1, snail2*; Fig. 1O-Q, Table S6). Definitive premigratory NC area was also enlarged (Fig. 1R,S). In contrast, neural plate specification, anterior-posterior regionalization (*sox2*, *otx2*, *hoxb9*) and non-neural ectoderm differentiation (*epidermal keratin*, abbreviated here to *ep. ker.*) were unaffected. We observed a transient and moderate enlargement of the *sox2*-positive area in mid-neurulas, probably related to the enlarged *sox2*-positive NB (Fig. 1U,W-Y, Table S6). Mesoderm formation seemed to be unaffected (*myod*; Fig. 1V). At tailbud stage (st.22-24), migrating NC streams were enlarged with similar ventral migration distance compared with the contralateral control side (Fig. 1T,Z). Together, *pfkfb4* expression and the PFKFB4 gain-of-function phenotype suggested a positive role in NC development. We did not observe ectopic expression of NC markers in the neural plate or the
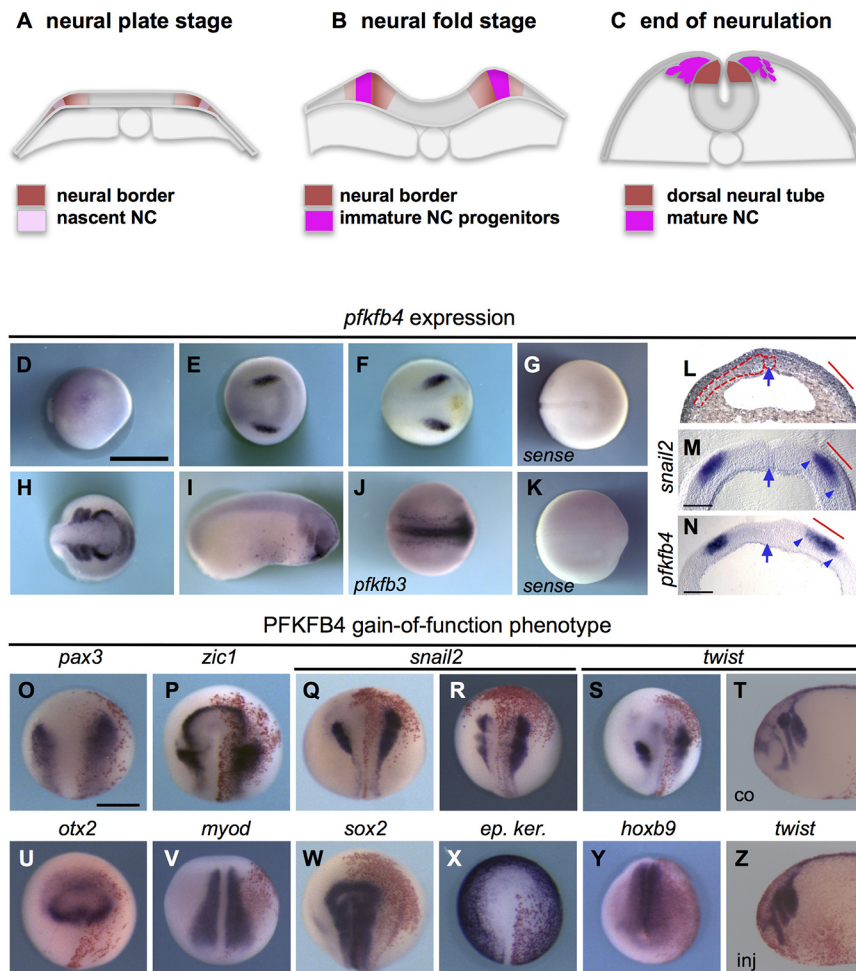

Fig. 1. PFKFB4 promotes NB and NC formation.
(A) NC is induced during neural plate stage (st.12.5-14). Expression of NB specifiers (red) is robustly established lateral to the neural plate, expression of early NC specifiers (*snail2*, *foxd3*) is faintly initiated (light pink). (B,C) During neural fold elevation (st.14-17, B), future NC cells progressively acquire their definitive specification and specific cellular properties (e.g. survival, expression of late NC specifiers, cadherin switch) enabling them to undergo EMT and migration (st.18-19, C). (D-F,H,I) *pfkfb4* is enriched in the NB/NC in neurulas and tadpoles. (J) *pfkfb3* is expressed in the neural tube. Sense probes are shown in G (*pfkfb4*) and K (*pfkfb3*). Neurula stages: late gastrula/early neural plate stage (st.12, D); end of neural plate stage (st.14, E); neural fold stage (st.16, F); neural tube closure/end of neurulation (st.19, H); tailbud stage (st.22, I). E-H,J,K: dorsal views, anterior to the right. D,I: side views. Scale bar: 1 mm. (L-N) Cross-sections through the mid-neurula anterior neural plate (st.14) show *snail2* and *pfkfb4* expression in NB/NC. (L) The notochord, neural plate and paraxial mesoderm are outlined on Hematoxylin and Eosin-stained sections. (M,N) Vibratome sections. Arrow indicates the midline. Arrowheads indicate the st.14 NB (red bar). Scale bars: 200 μm. (O-S) *pfkfb4* gain-of-function expanded the st.14 NB (O,P) and premigratory NC (st.14, Q; st.18, R, S). Migrating NC streams were expanded (st. 22-24, T, Z). In contrast, pan- or regional neural plate (*sox2*, *otx2*, *hoxb9*), ectoderm (*ep. ker.*) or paraxial mesoderm (*myod*) markers were unaffected (U-Y). O-S,U-X: dorsal views; T,Z: side views; Y: dorsal-posterior view. Scale bar: 500 μm. co, control side; inj, injected side. Phenotype scores are shown in Table S6.

non-neural ectoderm, suggesting that PFKFB4 was not sufficient to alter specification of adjacent ectoderm cells.

Moderate PFKFB4 depletion affects craniofacial development *in vivo*

To deplete PFKFB4 in gastrulas, we previously used a splice-blocking morpholino oligonucleotide (PFKFB4MO; Pegoraro et al., 2015), using 20 ng per blastomere in 2-cell-stage embryos. *pfkfb4* mRNA levels were decreased by 60% (hereafter called 'severe depletion'). Phenotypes were validated using ATG-targeting and a mismatch morpholino, dose-response experiments and rescue experiments (Blum et al., 2015). Severe depletion caused a developmental blockade before neural fold stage; all dorsal ectoderm cells remained in an immature progenitor status and further specification was blocked. Here, in order to analyze later PFKFB4 functions during NC formation, we used two strategies to bypass this early developmental arrest. First, we used low-level PFKFB4 depletion, which does not block ectoderm global developmental progression and allows neurulation to proceed. Second, using photo-inducible morpholinos, we controlled the timing of PFKFB4 depletion in order to avoid early development arrest.

Based on *pfkfb4*-enhanced NC expression, we hypothesized that NC development required maintenance of high PFKFB4 levels, whereas other tissues may develop normally under mild PFKFB4 depletion conditions. Using decreasing PFKFB4MO doses, we created mild hypomorph conditions by injecting 5 ng of morpholino (MO) into one dorsal-animal blastomere, at the 4-cell stage or any equivalent combination at other developmental stages, resulting in about 35% decrease in *pfkfb4* mRNA levels (Fig. 2A). We monitored craniofacial morphology and pigmentation phenotype of st.45 tadpoles (Fig. 2B-E, Table S7). Low-level depletion resulted in morphologically normal gastrulation and neurulation but caused a significant size reduction of head structures on the injected side, compared with the uninjected side (Fig. 2B). Pigment cells appeared to be unperturbed. Lower morpholino doses (2.5 ng or 1 ng in one of four blastomeres) did not significantly alter embryo morphology. Higher doses caused early death of the injected cells (this apoptosis was rescued by adding *pfkfb4* mRNA as described by Pegoraro et al., 2015). With the low-level PFKFB4 depletion, we confirmed that injected cells were not subjected to increased cell death compared with control cells in the vast majority of the embryos (Fig. S3). Moreover, neither ventral injections of PFKFB4MO nor dorsal injections of a non-related MO (even at high doses) caused cell death, excluding the possibility that cell death was merely due to MO injection (Fig. S3). Therefore, NC development was specifically affected by low-level depletion of PFKFB4. Using these hypomorph PFKFB4 conditions, we could explore the roles of PFKFB4 in NC formation *in vivo*. All further experiments, except for photo-morpholino experiments, were conducted using this low MO concentration.

The NC generates craniofacial skeleton, mesenchyme and soft tissues around the eyes. Following moderate PFKFB4 depletion, dorsal and ventral craniofacial structures were smaller. On the morphant side, branchial cartilages were strongly reduced whereas Meckel's and ceratohyal cartilages were moderately diminished (Fig. 2C-E). Eyes were also affected, with grossly normal shape but reduced size. As *pfkfb4* is present at low levels in the early neural plate (Fig. 1), this could be due to a cell-autonomous defect in the optic vesicles forming from the neural plate. Alternatively, cranial neural crest cell (NCC) defects could influence the developing eye (Bailey et al., 2006; Lwigale, 2015). Hence, the NC-derived craniofacial
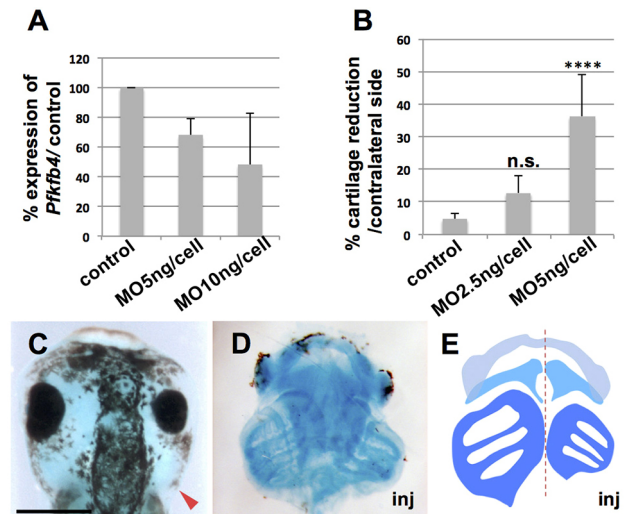

Fig. 2. Moderate PFKFB4 depletion results in severe craniofacial defects in tadpoles. (A) *pfkfb4* mRNA levels were quantified on neurula dorsal tissues by RT-qPCR. Injections at 'high concentration' (10 ng/cell in 4-cell-stage embryos) reduced *pfkfb4* levels by 52% and caused developmental arrest. A 'milder' concentration (5 ng/cell in 4-cell-stage embryos) decreased *pfkfb4* mRNA by 32% (low-level depletion), and allowed development to swimming tadpoles. (B-E) Craniofacial morphology in tadpoles st.45-46. Low-level PFKFB4MO depletion reduced the size of craniofacial structures on the injected side. The branchial arch cartilages area was severely diminished on the injected side. Lower doses did not significantly reduce cartilage area, or affect head morphology. n.s., not significant. (C) Head morphology, dorsal view; arrowhead indicates the injected side. (D) Dissected jaw and branchial arches cartilages, ventral view. inj, injected side. (E) Schematic of the image shown in D. Dashed red line indicates midline; light blue, Meckel's cartilage; mid blue, ceratohyal cartilage; dark blue, branchial cartilage. Scale bar: 500 μm. Phenotype scores are shown in Table S7.

structures were severely affected when PFKFB4 levels were downregulated moderately whereas most other structures were normal.

PFKFB4 depletion affects premigratory NC specification and NCC migration

We then investigated which steps of NC formation were affected by low-level depletion of PFKFB4. At early neural fold stage, *snail2* expression was very low to absent on the injected side (Fig. 3A,L, Table S8). This defect was a delay in expression, as by the end of neurulation most embryos expressed *snail2* at normal levels (Fig. 3B,L). In theory, delayed *snail2* activation could be followed by either later onset of the entire NC specification cascade or by globally defective NC development. To assess definitive NC specification at the end of neural fold stage, we analyzed expression of the late NC specification markers *sox10* and *twist1*. Although *sox10* was normally activated, *twist1* expression was severely defective and *hes4*, marking immature premigratory NC, was increased (Fig. 3C-E, Table S8). In contrast, neural ectoderm, non-neural ectoderm and paraxial mesoderm specification were unaffected (*sox2*, *ep.ker.*, *myod*; Fig. 3I-L, Table S8). Neural fold elevation was slightly delayed on the injected side, but neural tube eventually closed (Fig. 3G,I). Importantly, although some neural border markers were expressed normally at the time of neural tube closure (e.g. *msx1*; Fig. 3H), others were moderately (*zic1*) to strongly (*pax3*) increased suggesting that the NC cells had partially retained an immature NB-like character, at a developmental stage when they should have been specified into functional premigratory NC (Fig. 3F-H,L).
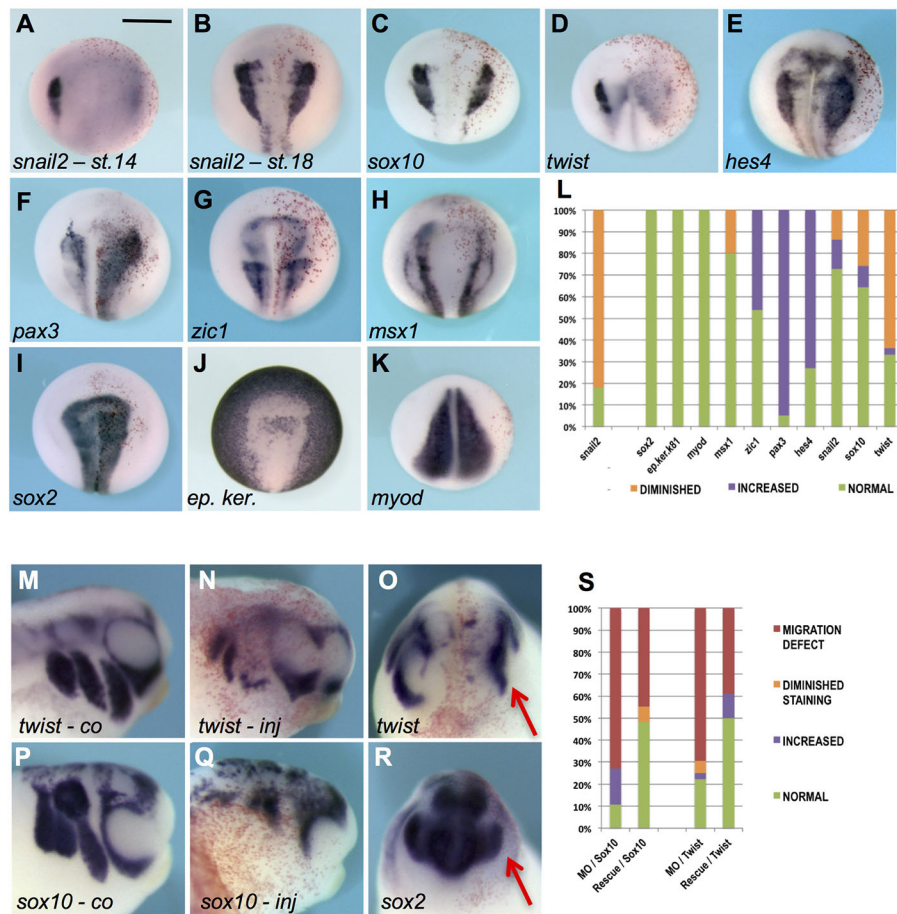
Fig. 3. PFKFB4 low-level depletion delays NC early specification, causes retention of NB character, and impairs NC late specification and migration. (A) At st.14, *snail2* expression was severely reduced, or abolished, on the injected side. (B) At st.18, sibling embryos had recovered *snail2* expression. (C,D) Whereas *sox10* expression was mainly unaffected, *twist1* was severely impaired. (E-H) In contrast, expression of the immature NC marker *hes4* was expanded, as were some NB markers, either strongly (*pax3*) or moderately (*zic1*). Other NB markers were unperturbed (*msx1*). (I-K) Neural plate (*sox2*), non-neural ectoderm (*ep. ker.*) and paraxial mesoderm (*myod*) seemed to be unaffected. A-K: dorsal views. (L) Percentage of embryos with each phenotype, i.e. diminished, increased or normal expression. *Snail2* score at st.14 is indicated as the first bar, then several gene scores at st.18 are indicated in the following ten bars. (M-R) St.24 tailbud embryos exhibited a severe NC migration defect (M-Q). *Sox2* expression appeared grossly unaffected, despite marginal reduction of optic vesicle size (R). The injected side (inj) is compared with the control side (co) in side views (M,N,P,Q, anterior to the right) or frontal views (O,R; red arrow on injected side). (S) Co-injection of *pfkfb4* mRNA with PFKFBMO rescued both *sox10/twist1* alterations of expression and NC migration defects in a significant proportion of the embryos, compared with PFKFB4MO injections alone. *sox10* and *twist1* expression were restored or increased a majority of the embryos. Scale bar: 500 µm. Phenotype scores are shown in Table S8.

During NC migration, low-level PFKFB4 depletion resulted in severely diminished *twist1* and *sox10* expression (Fig. 3M-S). Although the percentage of embryos with abnormal *twist1* expression was slightly lower than at the end of neurulation [Fig. 3S (st.24); Fig. 3L (st.18)], these results suggested that the gene expression defects observed in neurulas were not compensated for at the subsequent stages. At this stage, the central nervous system and the optic vesicle were grossly normal (*sox2*; Fig. 3R). When PFKFB4 morphant phenotype specificity was assessed, by co-injecting PFKFB4MO with *pfkfb4* mRNA, the morphant phenotype was rescued during NC specification and migration (Fig. 3S, Fig. S4; data not shown).

Altogether, these results indicated that a moderate loss of PFKFB4 activity resulted in a strong impairment of NC marker induction. The NC territory was established, identified by *sox10* expression and outlined by *msx1* expression (Fig. 3C,H). However, its specification was delayed at neural plate stage (*snail2*), and was incompletely compensated for at late neural fold stage (defective *twist1*, increased *hes4*); this was accompanied by the retention of NB-like character (increased *pax3*) in premigratory NC and was followed by defective expression of *sox10/twist1* in tailbud-stage embryos. As a result, fewer *twist1*- or *sox10*-positive cells populated the craniofacial areas. These alterations were sufficient to explain the morphological craniofacial defects observed at st.45 (Fig. 2). However, using the constitutively active PFKFB4MO, we could not distinguish between an early need for PFKFB4 during NC specification, causing defective NC migration, and a continuous need for PFKFB4 activity during NC specification and migration.

Inducible PFKFB4 depletion affects NC specification and its migration *in vivo*

To understand PFKFB4 function at each step of NC formation, we set up an inducible knockdown strategy, with a UV-cleavable sense morpholino (PFKFB4-PhMO) that blocked *pfkfb4* antisense-MO until UV exposure, in albino embryos. The uninjected side controlled for non-specific UV effects. As control, severe PFKFB4MO constitutive depletion led to abolished or severely decreased *twist1* expression (in 80% and 17% of embryos; Fig. 4A-C,H). PFKFB4-PhMO/MO co-injections efficiently blocked the severe morphant phenotype (uninduced embryos, u.i.): *twist1* was normally expressed in 60% of st.18 embryos. Despite minimal ambient light throughout experiments, we observed some leakage in the PhMO/MO u.i. condition, leading to 22.5% of embryos with severe decrease in *twist1* expression and 17.5% with mild defects. However, after UV exposure upon injection (a.i., illumination at the 4-cell stage), *twist1* expression decreased significantly on the injected side in 73% of embryos (Fig. 4H). The lower efficiency of the PhMO/MO a.i. condition compared with the constitutive PFKFB4MO phenotype, leading to only 26% of embryos with severe *twist1* blockade and 47% with mild defects, could be due to a partial *pfkfb4-PhMO* cleavage, leading to a hypomorph phenotype. Indeed, the embryos exhibited malformations similar to those observed at low doses with constitutive depletion (Fig. 3).

To study the role of PFKFB4 during NC specification, embryos were UV illuminated at the end of gastrulation (st.12.5), and analyzed at late neural fold stage (st.18). Before induction, development appeared normal (as assessed by *sox2* and *ep.ker.* expression, not shown). PFKFB4 knockdown from st.12.5 resulted
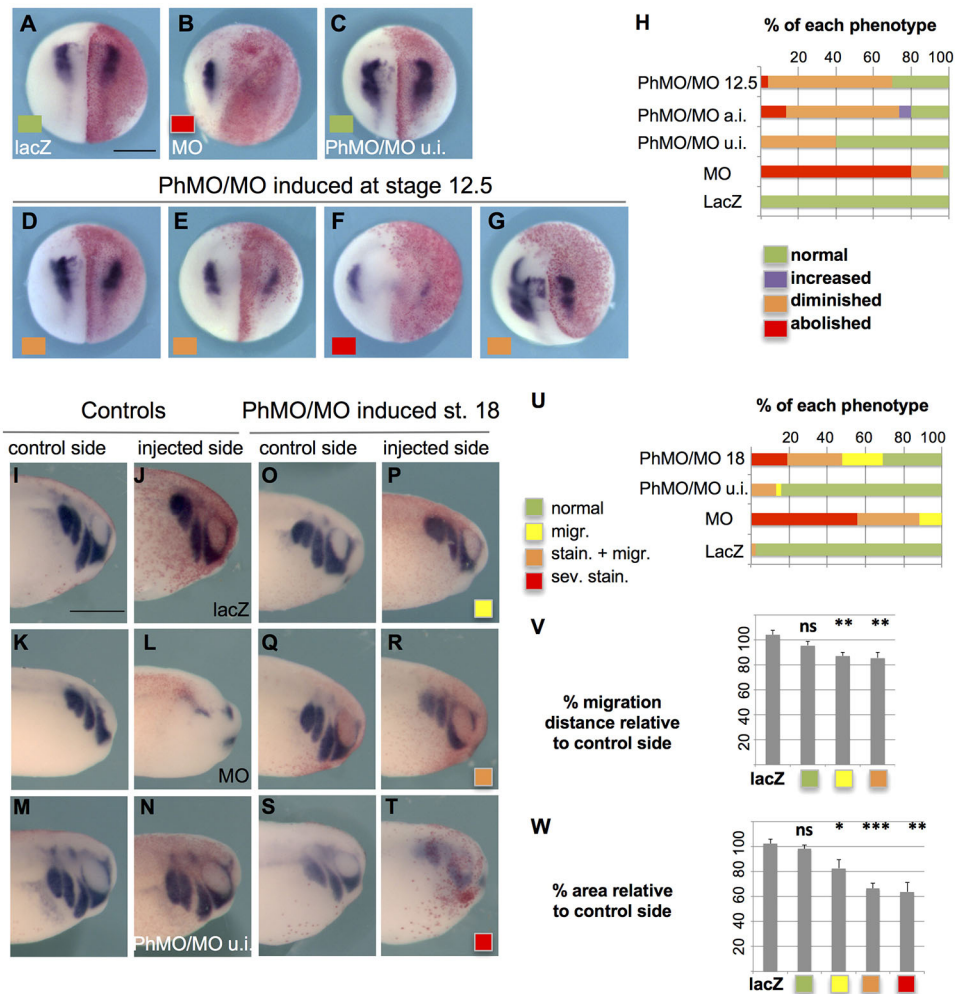
Fig. 4. Inducible depletion demonstrates that PFKFB4 has independent roles in NC specification and migration. We co-injected a UV-cleavable sense MO (PhMO) to block PFKFB4MO until the desired developmental stage and monitored *twist1* expression at st.18. (A-H) Strategy of phMO validation: *lacZ* control injections (A), unmasked PFKFB4MO, 'high' dose (B), PhMO/MO without UV illumination (C; uninduced, u.i.); UV illumination at early NC specification st.12.5 (D-G). D-F show two examples of diminished phenotype and one example of abolished phenotype at st.14; G shows an example of diminished phenotype at st.19. (H) Percentage of embryos with each phenotype, i.e. abolished, diminished, increased or normal *twist1* expression. *lacZ* injections did not alter *twist1* pattern. PFKFB4MO severely blocked *twist1* expression. *twist1* expression was decreased in PhMO/MO-injected embryos UV illuminated immediately after injection (a.i.) compared with uninduced PhMO/MO-injected embryos. *Pfkfb4* depletion, activated at st.12.5, decreased *twist1* expression strongly or moderately. This effect persisted until EMT and early NC emigration (G; st.20). (A-G): dorsal views. (I-W) To deplete *pfkfb4* during EMT/early migration, st.18 neurulas were UV illuminated and analyzed at tadpole st.24. *twist1* expression was normal in embryos injected with *lacZ* (I,J), or with PhMO/MO but not illuminated (M,N). Cells injected with PFKFB4MO alone died as expected (K,L). PhMO/MO-injected embryos UV illuminated at st.18 exhibited three phenotypes classes: 'migration' (O, P), 'staining and migration' (Q,R) and 'severe staining' defects (S,T). We compared the percentage of each phenotype (U), of migration distance (V) and of NC stream area (W; *twist1*-expressing area) with the contralateral side. Scale bars: 500 μm. All phenotype differences were statistically significant between illuminated PhMO/MO-injected embryos, and either *lacZ*-injected, or uninduced PhMO/MO-injected embryos (*$P<0.05$; **$P<0.01$; ***$P<0.001$; ns, not significant). Error bars represent s.e.m. Phenotype scores are shown in Table S9.

in a significant *twist1* downregulation (Fig. 4D-H) compared with injected but uninduced embryos. Therefore, PFKFB4 plays a specific role during NC specification, distinct from its early function on ectoderm patterning during gastrulation. Moreover, this effect mirrors the hypomorph phenotype observed with mild PFKFB4 depletion (Fig. 3).

PFKFB4 knockdown was then induced at late neural fold stage, as NC cells have completed specification, maturation and initiated EMT (st.18). Before illumination, development was mainly normal, despite slightly decreased *twist1* expression (u.i.; Fig. 4H). In st.24 tadpoles, we analyzed *twist1* expression, NC streams shape and migration distance from the dorsal midline. *twist1* expression was normal in embryos injected with *lacZ* alone (no MO) or PhMO/MO

uninduced, whereas the injected cells were lacking (eliminated after cell death) in PFKFB4MO-injected embryos (Fig. 4I-N,U). After photo-induction at st.18, *twist1* was significantly altered in 69% of embryos (Fig. 4O-U). For the milder phenotype ('migration', 21%), tadpoles presented a modestly reduced migration distance (13% reduction), with a robust *twist1* expression but smaller NC streams (17% area reduction). This limited effect was reproducible and statistically significant, compared with variations observed in *lacZ*-injected embryos or the injected embryos classified as normal (Fig. 4O,P,V,W). The second phenotype ('migration and staining', 28.5%) presented similarly reduced migration distance (14% reduction) but more intense decrease in NC streams area (34% smaller) and lower *twist1* staining intensity (Fig. 4Q,R,V,W).

Finally, 19% of the embryos exhibited strongly reduced *twist1* expression ('severe staining defect'), with 36% reduced area, the low staining preventing measure of migration distance (Fig. 4S,T,V, W). Hence, depleting PFKFB4 after NC specification, at the time of EMT, affected *twist1* expression, the size of NC streams, and NC migration distance.

Together, these results demonstrated a requirement for PFKFB4 function at two successive and distinct steps of NC development: patterning of mature NC during neurulation and NC migration at tailbud stage. Moreover, these effects closely mimicked those observed after low-level depletion of PFKFB4.

PFKFB4 controls AKT signaling in premigratory NC
PFKFB4 regulation of glycolysis, as seen in adult cells, was not involved in late specification of NC, as glycolysis blockade during neural fold stage did not alter *twist1* expression (Fig. S5; other markers not shown). In order to understand how PFKFB4 might affect late specification of NC, we assessed cell signaling parameters and cell proliferation in premigratory NC. In gastrulas, PFKFB4 levels impact PI3K-AKT signaling. Here, to address precisely the level of AKT signaling in developing NC progenitors, we dissected out either the neural border territory at the end of neural plate stage, or the premigratory cranial NC at the end of neural fold stage, and measured phospho-Ser473-AKT levels in control and PFKFB4 hypomorph conditions. AKT signaling was specifically decreased in morphant NC progenitors compared with controls (Fig. 5A).

AKT signaling regulates many aspects of cell homeostasis, including cell proliferation. We next wondered if the rate of cell proliferation was affected in morphant NC, and if the pool of *cmyc*-positive NC stem cells was normal (Bellmeyer et al., 2003). After 5-ethynyl-2′-deoxyuridine (EdU) incorporation, we observed normal cell proliferation on the morphant side (Fig. 5B). *cmyc* expression was normal on the morphant side, whereas *twist1* was defective in sibling embryos (Fig. 5C,D). Together, these results suggested that the morphant territory generates a rather normal pool of NC stem cells, suggesting that the phenotype relies on genuine patterning defects within a partially specified NC domain.

To assess whether diminished AKT signaling was sufficient to affect NC specification and maturation, and to phenocopy the morphant phenotype, we treated embryos with a PI3K-AKT inhibitor (LY294002, 40-80 μM). As a comparison, we used a MAPK/ERK inhibitor (UO126, 40-80 μM) because both AKT and MAPK signaling pathways are often activated downstream of tyrosine kinase receptor signaling. Each treatment was checked for inhibition of p-ERK and p-AKT (on whole embryo lysates, not shown). Embryos were treated exclusively during the neural fold stage (from st.14 to st.18). Inhibiting PI3K-AKT signals blocked *twist1* but not *cmyc* induction. In contrast, the ERK inhibitor had no effect on expression of either gene (Fig. 5E-H). This result showed that AKT signaling is specifically needed during the last phase of premigratory NC maturation. When AKT function was disrupted, a normal pool of *cmyc*-positive NC stem cells formed but they failed to express the late NC specifier *twist1*.

Finally, when a constitutively active form of AKT was co-injected with PFKFB4MO, *twist1* specification defects were rescued, demonstrating that the main cause of the PFKFB4 morphant phenotype prior to migration was altered AKT signaling (Fig. 5I,J).

PFKFB4 depletion affects NC EMT and migration in a cell-autonomous manner
To understand the defects during NC EMT and migration upon PFKFB4 low-level depletion, we reasoned that morphant NC cells,
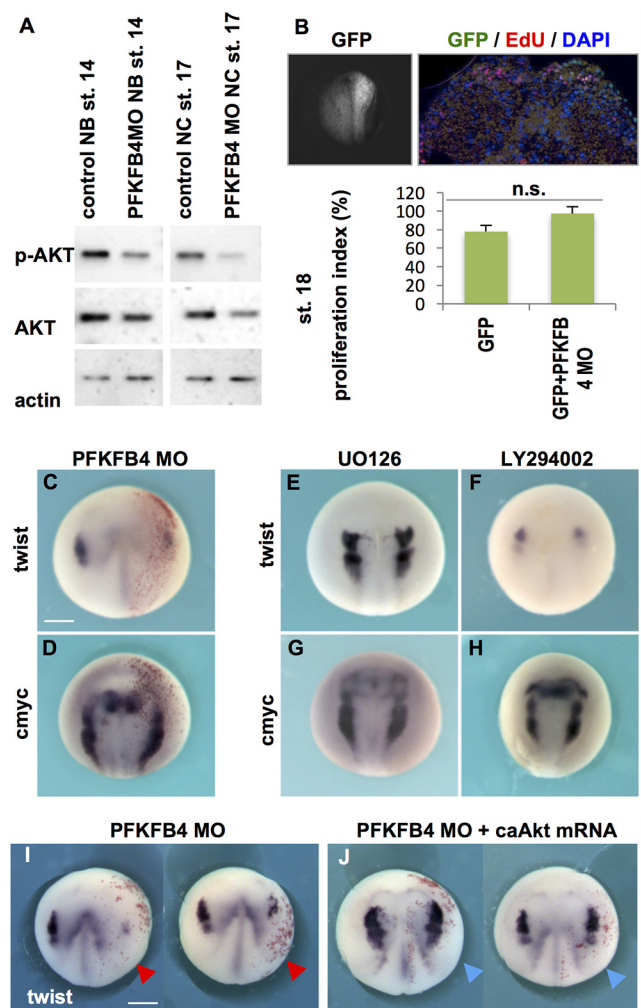

Fig. 5. AKT signaling mediates the effect of PFKFB4 on premigratory NC maturation. (A) In embryos, PFKFB4 regulates AKT signaling in addition to glycolysis. Dissected morphant st.14 NB or st.17 NC displayed decreased AKT signaling. (B) AKT regulates many aspects of cell homeostasis including cell proliferation, cell survival, and cell metabolism. However, EdU incorporation showed that cell proliferation rate was normal after PFKFB4MO injections. Error bars represent s.e.m. n.s., not significant. (C,D) PFKFB4MO affected late NC specifier *twist1* expression, whereas the NC stem cell marker *cmyc* was normally activated. (E-H) Pharmacological treatment during neural fold stage (st.14-18) showed that blocking MAPK signaling (E,G) did not affect NC development, but blocking PI3K-AKT signaling (F,H) affected *twist1* but not *cmyc*, thus phenocopying the PFKFB4MO effect. (I,J) Co-injection of PFKFB4MO with a constitutively AKT (*caAkt*; blue arrows) rescued the morphant *twist1* phenotype (red arrowheads): two sibling embryos for each injection are shown. St.18 *pfkfb4* morphants presented diminished *twist1*. In contrast, siblings co-injected with PFKFB4MO and *caAkt* mRNA had normal *twist1* expression in the majority of cases. Scale bars: 500 μm. Phenotype scores are shown in Tables S8, S13.

with delayed or incomplete specification (Fig. 3), might require a longer time than wild-type NC to mature and undergo migration. Additionally, interactions between the NC and its *in vivo* environment are essential for migration. Using the more robust pigmented frog embryos, we challenged the ability of morphant NCCs to migrate in a wild-type host environment (Fig. 6). We implanted GFP-labeled premigratory morphant NC into a stage-matched wild-type host and followed cell migration *in vivo*. In contrast to the control wild-type grafts, which healed within 20 min after transplantation, the morphant tissue healed with difficulty:
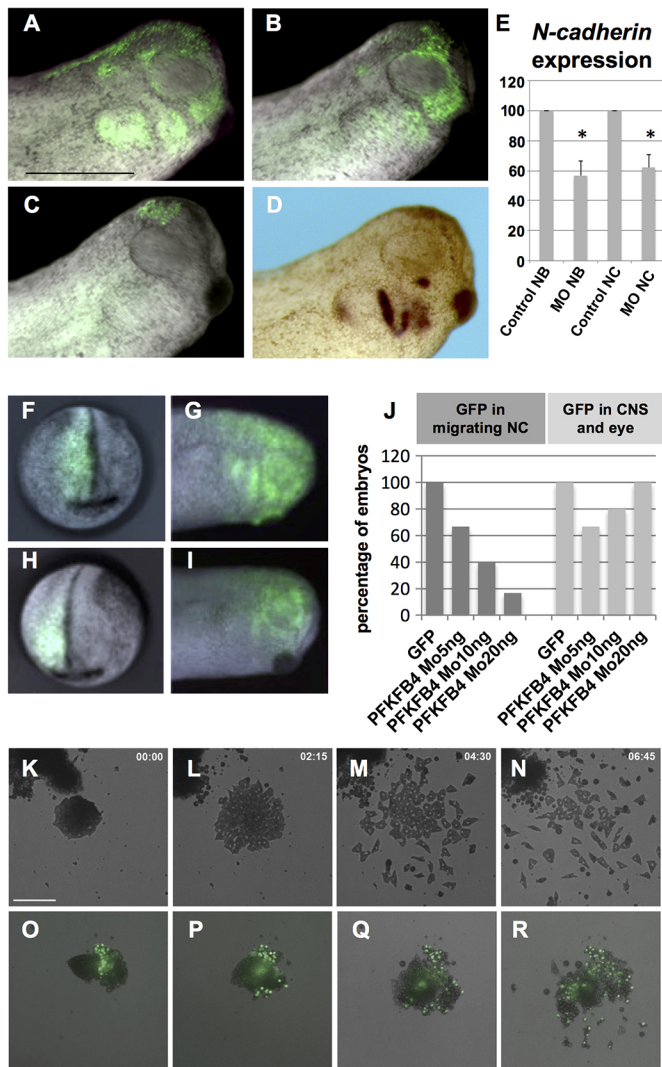
Fig. 6. PFKFB4 morphant NC progenitors fail to undergo EMT and migration. (A,B) When transplanted into a wild-type host embryo, GFP-labeled wild-type NC efficiently migrates and populates the host branchial arches, regardless of the size of the grafted tissue, i.e. large graft (A) or small graft (B). Scale bar: 500 μm. (C,D) In contrast, PFKFB4 morphant NC exhibited defective healing, resulting in small-size grafts, which yielded few, if any, migratory NCC into the host craniofacial area. (C) Small graft without migratory cells; (D) small graft with few cells reaching the branchial arches. In D, *gfp* was detected by WISH to enhance individual cell visualization. (E) The effect of PFKFB4MO on *N-cadherin* expression (RT-qPCR on dissected explants), either prior to EMT (NB, st.14), or in premigratory NC (st.17). Error bars represent s.e.m. *$P \leq 0.05$. (F-J) Wild-type (F,G; *gfp* only, no MO) or morphant (G,I; MO 10 ng) cells were lineage traced *in vivo*, on embryos injected in the prospective neural fold unilaterally. At tailbud stage, control cells (G) efficiently populated branchial arches and were also found in brain and eye (J). In contrast, morphant cells failed to populate branchial arches (I) in a dose-dependent manner (J), but were normally distributed in the brain and eye (J). (K-R) NB tissue was dissected prior to EMT (st.14) and plated onto fibronectin. Cell behavior was followed by time-lapse videomicroscopy. Wild-type NC (K-N) adheres efficiently, and undergoes EMT (L), cell scattering and migration (M, N). Morphant NC (O-R) presented poor adherence, delayed (P) and inefficient EMT (Q), and few emigrating cells (R). Time after plating is indicated (h:min). Scale bar: 160 μm. Phenotype scores are indicated in Table S10.

most of the donor tissue failed to adhere to the host tissues, even as long as 2 h post-grafting (not shown). Moreover, after healing, the vast majority of the grafted morphant cells failed to migrate, although occasional cells could be traced in the mandibular arch

area (Fig. 6C,D, compare with wild-type cells in 6A,B). This phenotype was qualitatively similar to the defects observed in the morphant embryos (Fig. 4), either with constitutive or inducible morpholinos. In this transplantation assay, however, the lack of migration was observed in a higher number of cases, possibly because of the additional healing defect revealed by the assay. This challenge revealed that PFKFB4 morphant cells displayed altered healing and survival ability upon EMT and migration.

We further analyzed the fate of the morphant cells *in vivo* with another strategy. In order to avoid interference from altered healing properties, we traced the injected cells with *gfp* mRNA co-injected with PFKFB4MO, by targeting dorsal-animal blastomere D1.2, which mostly forms dorsal neural tube and NC progenitors (Moody, 1987), by injecting between the 8-cell stage and the 16-cell stage. We followed the fate of NC progenitors, by selecting embryos with GFP-positive premigratory NC at the end of neurulation (st.18; Fig. 6F-H). In these conditions, without further experimental manipulation of the injected cells, we found that the control cells undergo EMT, migrate and populate efficiently craniofacial areas as expected, whereas morphant cells failed to do so in a dose-dependent manner. In contrast, the morphant cells contributed to brain and eye as efficiently as did control cells (Fig. 6G,I,J). We concluded that the defective NC specification and maturation, observed at st.18, was not compensated for later on, even when morphant cells face a wild-type environment, and that a lower PFKFB4 activity resulted in a cell-autonomous alteration of the ability of the NC to undergo EMT and migration *in vivo*.

To understand the cellular and molecular basis of morphant NC phenotype, we tested adherence, EMT and migration on fibronectin *in vitro* (Fig. 6K-R). This assay was carried out using earlier tissue than in previous publications, i.e. using neural border at st.14 instead of premigratory NC st.17-18, which has already started EMT. Doing so allows separate visualization of adherence a few minutes after plating, then EMT about 2 h after plating, and finally cell migration on the fibronectin substrate starting 3.5-4 h after plating (Fig. 6K-N). Morphant neural folds were thus dissected out at the end of neural plate stage (st.14). They failed to adhere efficiently on fibronectin, did not undergo EMT (Fig. 6O,P) and migrated poorly (Fig. 6Q,R), whereas wild-type neural folds adhered, underwent a very clear EMT (Fig. 6K,L), dispersed and actively migrated (Fig. 6M,N). A key parameter for NC EMT is the upregulation of *n-cadherin* (*cadherin 2*) expression prior to EMT (Theveneau and Mayor, 2012). We found that *n-cadherin* expression levels were significantly lower in morphant NB (st.14) and NC (st.18) compared with stage-matched controls (Fig. 6E).

We concluded that lower PFKFB4 activity resulted in premigratory NC with defective *n-cadherin* levels. These cells were unable to undergo EMT on a fibronectin substratum *in vitro*, and exhibited poor ability to adhere, heal or migrate upon grafting in wild-type host environment *in vivo*. The morphant cells remained integrated into adjacent tissues such as central nervous system or eye. These altered capacities were sufficient to explain the late phenotype in tadpoles, with underdeveloped craniofacial structures.

At tailbud stage, PFKFB4 depletion alters both glycolysis and AKT signaling, which together impact NC migration

PFKFB4 depletion decreased glycolysis in embryos (Fig. S5). To understand the PFKFB4 depletion phenotype during NC migration, we blocked either glycolysis or AKT signaling from EMT stage (st.18) to migration into branchial arches (st.24) (Fig. 7, Fig. S6). Glycolysis was blocked using 2-deoxyglucose (2DG), a non-hydrolysable glucose. The PI3K inhibitor LY294002 was used at
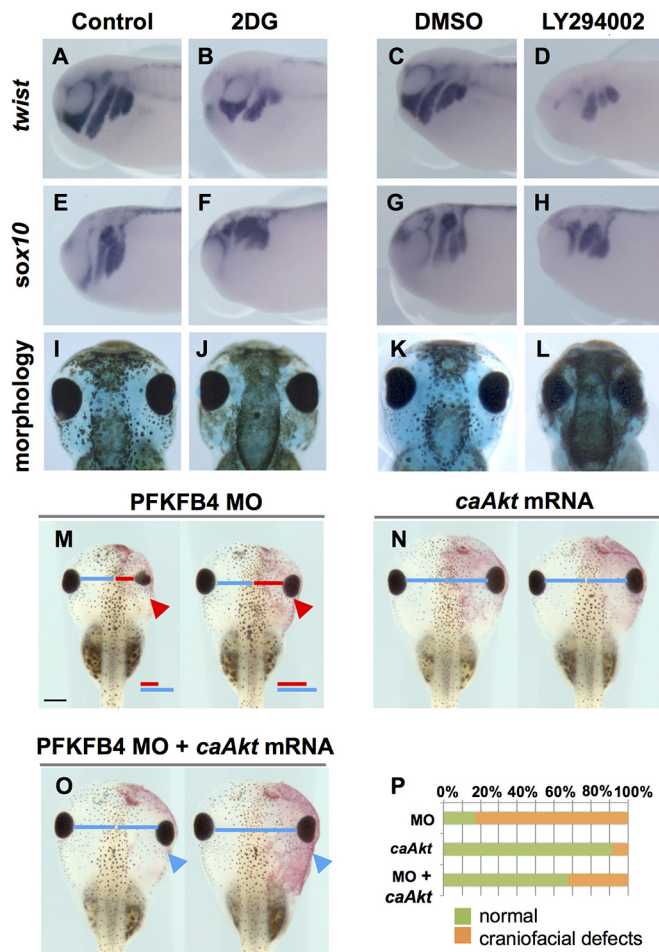
Fig. 7. Glycolysis and PI3K-AKT signaling impact NC migration similarly to PFKFB4 low-level depletion, and activating AKT signaling rescues PFKFB4 downregulation. (A-H) When glycolysis (2DG) or PI3K-AKT pathway (LY294002) were blocked during EMT and migration (st.18-24) both treatments severely affected NC migration at st.24 (as revealed by *twist1* and s*ox10* expression). (I-L) At st.45, tadpoles treated during NC migration then grown in control medium, exhibited general head morphology defects, including eye defects and smaller branchial cartilages. (I,K) Sibling controls; (J) 2DG; (L) LY294002. A-H show side views; I-L dorsal views. (M-P) At tadpole st.45, morphant sides were severely affected (M,P), whereas activation of *Akt* signaling (N,P) did not affect overall craniofacial morphogenesis. Tadpoles co-injected with PFKFB4MO and *caAkt* (O,P) were largely rescued, with 66% of embryos with injected side symmetrical to contralateral side. (M) Red bar indicates eye distance from the midline on the morphant side; blue bar indicates control distance. Both bars are aligned below for comparison. (N,O) On both sides, the same blue bar measures eye distance from the midline. Arrowheads indicate the injected side. Scale bar: 500 μm. Phenotype scores are shown in Tables S11, S12.

various doses to block PI3K-AKT signaling. The efficiency of each treatment was monitored (Fig. S5). We found that both glycolysis and AKT phosphorylation blockade from st.18 to st.24 resulted in severe disruption of NCC migration, (*twist1*, *sox9*, *sox10*; Fig. 7, Fig. S6). The effects of LY294002 were dose dependent (not shown). Whereas glycolysis blockade seemed to mainly affect NC streams morphology, AKT inhibition also affected general embryo development (not shown). In order to test for delayed NCC migration and for general treatment toxicity, embryos were transferred to drug-free medium from tailbud st.24 until late tadpole st.45. Under these conditions, potential delays would be compensated for, whereas general toxicity would lead to embryo

death. Here, embryo survival was normal. St.45 craniofacial morphology was analyzed. Relative to body size, heads were smaller and visceral cartilage elements were severely underdeveloped, as observed upon PFKFB4 depletion, especially after AKT signaling blockade. Interestingly, combining both glycolysis and AKT blockade led to a stronger craniofacial phenotype, suggesting cooperation of the two processes (Fig. S6). We concluded that blocking AKT signaling or, with less efficiency, blocking glycolysis, phenocopied the PFKFB4 morphant phenotype during NC migration. Both AKT signaling and glycolysis are thus needed for a large number of NCCs to populate the branchial arches and head structures.

Because AKT blockade seemed to be the most effective in mimicking PFKFB4 depletion, we attempted to rescue the craniofacial phenotype by co-injecting a constitutively active *Akt* mRNA (*caAkt*) with PFKFB4MO. By st.45-46, we observed that constitutive activation of AKT signaling alone did not affect craniofacial development (Fig. 7N,P). Whereas morphant-injected sides were severely reduced in size (Fig. 7M,P), most tadpoles co-injected with PFKFB4MO and *caAkt* were symmetrical (Fig. 7O,P). This experiment demonstrated that the defects of NC craniofacial derivatives observed upon PFKFB4 depletion were largely due to loss of AKT phosphorylation and were efficiently compensated for by restoring active AKT signaling.

NC-GRN regulators control *pfkfb4* activation at the neural–non-neural border

Finally, we analyzed *pfkfb4* upregulation at the edges of the neural plate. We investigated whether the NC-GRN actors actively controlled *pfkfb4* expression, as they do for *snail2*, either during early *pfkfb4* activation at the end of neural plate stage, or in premigratory NC. We used MO-mediated depletions with well-established morpholinos, dominant-negative constructs (Fig. 8) or gain-of-function experiments (Fig. S7). First, the secreted NC inducers, including WNT and FGF8 signals as well as modulators of BMP signaling, affected *snail2* and *pfkfb4* expression similarly (Fig. 8A-L, Fig. S7). Second, we found that the key transcription factors acting at the NB to specify NC, PAX3 and TFAP2a, were also essential for normal *snail2* and *pfkfb4* expression (Fig. 8M-T, Fig. S7). In addition, the NC specifier SOX9 was needed for expression of both genes at the NB and in premigratory NC (Fig. 8U-X). All these results indicated that increased *pfkfb4* expression in the NC progenitors is actively promoted by NC-GRN regulators, as for more classical partners of the network (e.g. *snail2*). Thus, our results show that the key function of PFKFB4, which mainly relies on ensuring proper AKT signaling in NC progenitors, is encoded within the NC-GRN. PFKFB4 could be a major intermediate actor in NC control by WNT-FGF-BMP signals.

DISCUSSION
This study provides evidence that PFKFB4 is required continuously during several key steps of NC formation: during premigratory NC maturation at neural fold stage, and during NC migration towards the craniofacial prominences at tailbud stage. PFKFB4 depletion causes hypomorphic craniofacial structures. The major transcription factors and signaling pathways that control the NC-GRN control *pfkfb4* activation in NC progenitors during neural fold stage, i.e. during the phase of NC maturation. In turn, PFKFB4 controls AKT signaling activity in NC, which is essential for NC maturation and migration. PFKFB4 is a known glycolysis regulator, and its depletion in neurulas affected glycolysis. However, at neural fold stage, glycolysis is not required for NC patterning. In contrast, at
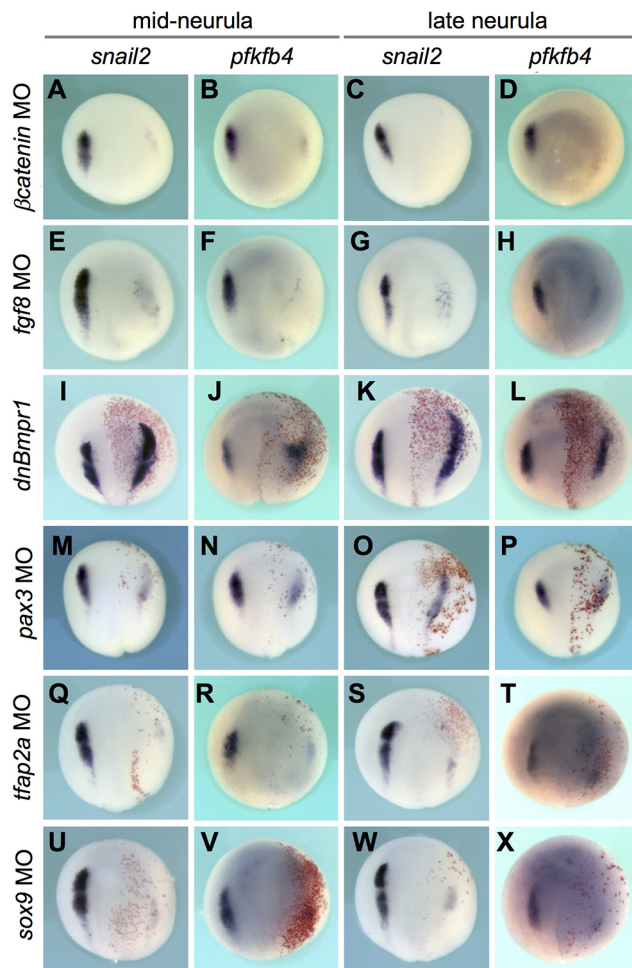
Fig. 8. *Pfkfb4* activation during neural fold stage is regulated by the NC-GRN. (A-X) Unilateral depletion of members of the NC-GRN modulated *pfkfb4* activation at the NB (st.14) and NC (st.18). (A-H) Blockade of WNT and FGF signaling strongly decreased *snail2* and *pfkfb4* expression. (I-L). Conversely, BMP signaling downregulation upregulated *snail2* and *pfkfb4* expression, laterally to the NB. (M-T) Knockdown of the NC specifiers PAX3 and TFAP2a resulted in loss of *snail2* and *pfkfb4*. (U-X) Knockdown of the NC specifier SOX9 depleted *snail2* and *pfkfb4*. Dorsal views, injected side on the right. Scale bar: 500 µm. Phenotype scores are shown in Table S13.

tailbud stage, both AKT signaling and glycolysis are important parameters to ensure NC migration. Finally, restoring AKT signaling compensates for PFKFB4 depletion and results in normal craniofacial development. This indicates that the crucial action of PFKFB4 on NC development is mainly mediated by its effect on AKT signaling (Fig. 9).

The enzyme PFKFB4 is an integral partner of the NC-GRN. Although it is ubiquitously expressed in the dorsal ectoderm at gastrulation stage (Pegoraro et al., 2015), we found that, during neurulation, *pfkfb4* expression is upregulated in immature NC progenitors, starting at neural fold stage. *Pfkfb4* is further expressed in the NC initiating their migration (Fig. 1). We have shown that the major NC-GRN regulators, including secreted inducers, NB specifiers and NC specifiers, control *pfkfb4* expression in the neural folds (Fig. 8). Moreover, depletion of PFKFB4 did not prevent expression of NB specifiers but led to delayed or decreased expression of early (*snail2*) and late (*twist1*) NC specifiers (Fig. 3). According to the hierarchical model of the NC-GRN, this indicated that PFKFB4, although not a transcription factor, acts as an NC

specifier (Betancur et al., 2010; Milet and Monsoro-Burq, 2012). The maintenance of *pfkfb4* expression in NC could further involve NC-GRN actors. We have shown that PFKFB4 was needed reiteratively during NC specification and migration (Figs 4 and 6). Likewise, WNT and TFAP2a function are also needed at successive steps of NC formation (LaBonne and Bronner-Fraser, 1998; Monsoro-Burq et al., 2005; Simões-Costa et al., 2015; Luo et al., 2003; de Crozé et al., 2011). Both WNT signals and TFAP2a activate *pfkfb4* expression during NC specification, suggesting that they could potentially sustain its expression also during later NC development.

Our data suggest that the main function of PFKFB4 upregulation in premigratory and migratory NC is to ensure optimal AKT signaling levels in these cells (Figs 5 and 7). We also show that blocking AKT signaling in temporally controlled conditions affects NC specification and migration independently (Figs 5 and 7). In mouse embryos, a recent study also demonstrated the importance of AKT signaling for NC migration: *Specc1l* mutants or knockdowns exhibit defective neural tube closure and cranial NC migration, with decreased phospho-AKT levels. In this context also, activating PI3K-AKT signaling rescued the phenotype (Wilson et al., 2016). Together, these data suggest that the acute need for optimal AKT signaling during NC migration might be conserved in amniote and non-amniote vertebrates.

The regulation of NC early development by PFKFB4 and AKT was essential to shape the embryonic head. We propose that it ensures that numerous NCCs populated the branchial arches, and differentiated into cartilage elements of appropriate size rather than impacting the morphogenesis of these elements (Figs 2 and 7). When inducible depletion was performed during NC migration only, cells eventually migrated almost down to the target tissues, but in smaller numbers (Fig. 4). Neural tube closure and craniofacial defects are an acute societal issue for human health. Hypomorphic craniofacial structures, especially of the jaw, are observed in many human syndromes, but are not yet linked to specific mutations (reviewed by Heike et al., 1993). Our study shows that impaired AKT signaling, specifically in the NC progenitors by means of PFKFB4 depletion, results in smaller jaw and branchial arches structures. This could happen because defects arose at time of NC specification, or during its migration. Our results thus show that even modest reduction of PFKFB4 levels, or of AKT signaling, when applied during developmental periods corresponding to crucial steps of NC development, results into severe craniofacial defects. This study highlights the importance of a strict temporal schedule during the NC developmental cascade. This schedule culminates with the EMT and migration onset of mature NC cells associated with neural tube closure. Optimal AKT signaling, regulated by high PFKFB4 levels, ensures that no delay in this developmental cascade occurs, that immature progenitor (NB-like) characters are not retained, and that the ultimate molecular switches (*twist1* and *n-cadherin* expression) are activated in a timely manner, allowing NC to undergo EMT upon neural tube closure. Later on, PFKFB4 and AKT signaling further optimize the efficiency of NC cell migration towards the branchial arches. Similarly, AKT signaling was recently shown to upregulate *n-cadherin* and control NC migration downstream of PDGF-A/PDGFRa (Bahm et al., 2017). This suggests that various cell inputs use AKT signaling as a hub to control NC formation.

During NC migration, our results outlined a potential link between PFKFB4, AKT and glycolysis, because AKT activation rescued the global *pfkfb4* morphant phenotype (lower AKT signaling and lower glycolysis rate; Figs 5 and 7). We conclude
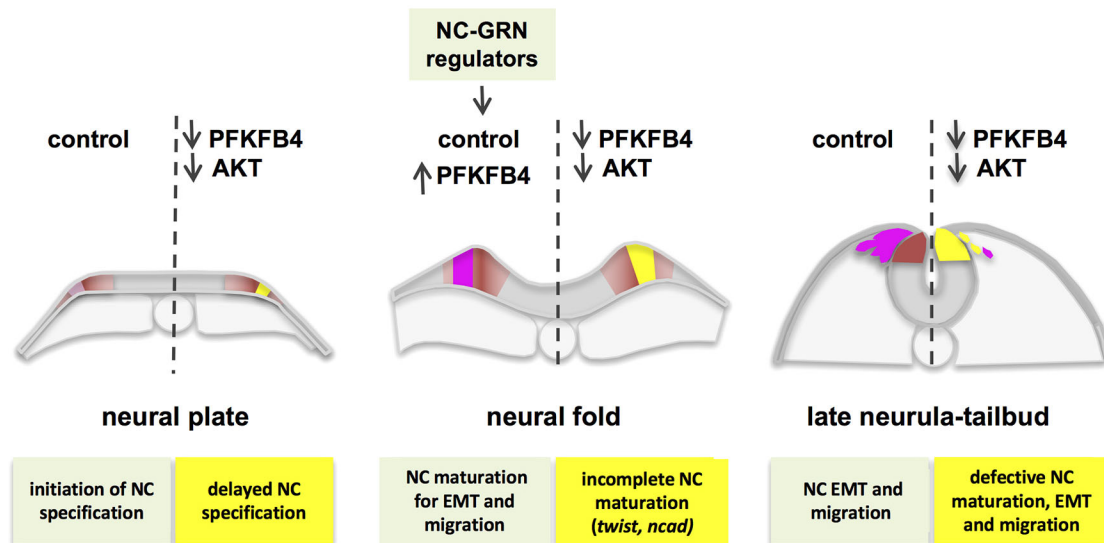
Fig. 9. Model of PFKFB4-controlled AKT signaling in NC maturation, EMT and migration. During neurulation, in controls (left side), NC is induced at the neural plate stage with weak *snail2* expression. This induction is then strengthened during neural fold stage, under the action of the NC-GRN, which notably activates *pfkfb4* expression in NC progenitors. This second phase allows acquisition of cellular ability to undergo EMT and migration upon neural tube closure. When AKT signaling is defective (right side), either after PFKFB4 low-level depletion, or using pharmacological inhibitors, delays in NC specification cascade occur, incomplete maturation is observed, and NC fails to undergo EMT. When PFKFB4 and AKT functions are prevented after EMT, fewer NCCs migrate resulting into reduced craniofacial skeletal elements. Hence, each step of NC early development relies upon continuous and elevated AKT signaling, sustained by PFKFB4, itself triggered by the NC-GRN.

that AKT compensates for all aspects of PFKFB4 depletion, directly or indirectly. In adult cancer cells and stem cells, PI3K/AKT signaling regulates glycolysis, which controls tumor cell motility (Han et al., 2013; Ito and Suda, 2014; Courtnay et al., 2015). This mechanism could be involved in NC development, as forced AKT signaling rescues the PFKFB4 phenotype. Comparison with cancer cells further highlights potential common mechanisms. In tumors, glycolysis enzymes are multifunctional regulators, which impact on cell physiology in addition to their role in glycolysis. For example, alpha-enolase (enolase 1) regulates PI3K-AKT signaling and downstream cell EMT regulators such as snail 1 and N-cadherin in lung cancer (Fu et al., 2015). PFKFB3 controls PI3K-AKT in human osteoarthritis cartilage, in adipocytes and in cancer cells (Trefely et al., 2015; Qu et al., 2016). It has been proposed recently that increased aerobic glycolysis in tumor cells (Warburg effect) promotes cell survival and cell cycle by stimulating IGF/AKT signaling, in addition to its role in cellular energy and metabolic intermediate production (Trefely et al., 2015). Our findings highlight a novel embryonic process, essential for NC EMT and migration, that parallels some mechanisms of cancer progression. It was shown that migrating NC cells displayed increased resistance to multiple cell stresses (Vega et al., 2004), ensuring their optimal long-distance travel throughout various embryonic environments. Altogether, our findings show how these properties are acquired and sustained, during and after premigratory NC maturation, and how they are encoded in the NC-GRN, using the unconventional function of a glycolysis regulator to control AKT signaling.

MATERIALS AND METHODS
Embryos, microinjection, NB culture and NC grafts
Pigmented and albino *Xenopus laevis* embryos were obtained and staged using standard procedures (Sive et al., 2010; Nieuwkoop and Faber, 1994). European and National Regulation for the Protection of Vertebrate Animals used for Experimental and other Scientific Purposes were strictly applied (license #C91-471-108, Direction Départementale de Protection de la Population, Courcouronnes, France). MOs or mRNAs were co-injected with *NLS-lacZ* mRNA or *histone2B-gfp* mRNA for lineage tracing. β-Galactosidase activity, revealed in red, marked the injected side. Embryos were injected unilaterally for whole-mount *in situ* hybridization/morphology or on both sides for western blot and RT-qPCR. NB and NC culture/grafting experiments were carried out as described by Milet and Monsoro-Burq (2014).

Plasmids and morpholinos
mRNAs were obtained *in vitro* (mMessage mMachine SP6 or T7 kits, Ambion). UV-cleavable photomorpholino (PhMO) experiments were performed on albino embryos (molecular ratio of sensePhMO/splice-blockingMO=1.25). PhMO cleavage was induced by a 15 min UV exposure using a HBO 103W/S source. Plasmids and MOs are listed in Tables S1 and S2.

Pharmacological treatments
Glycolysis, MAPK and PI3K-AKT signaling were inhibited using 2-deoxyglucose, UO126 or LY294002 (all from Sigma), respectively, on batches of 50 sibling embryos. Lactate concentration was measured on 20-40 embryos (L-Lactate Kit, Abcam). Reagents are listed in Table S3.

Cell proliferation and cell death assays
Cell proliferation was assessed based on EdU incorporation 2 h after ventral injection of 1 mM EdU (Molecular Probes) into st.18 embryos. Embryos were injected unilaterally, either with *gfp* mRNA alone, or PFKFB4MO and *gfp* mRNA into 4-cell stage embryos. After st.18 EdU injections and fixation, embryos were cut as serial paraffin sections. A minimum of 130 cells in the territory corresponding to the NC was counted on the GFP-injected side, compared with the contralateral side. Cell death was assessed by activated caspase 3 immunostaining *in toto*. Reagents are listed in Tables S4 and S5.

Cartilage staining
Embryos were stained with 0.05% Alcian Blue, de-stained in ethanol, rehydrated and cleared with 4% KOH followed by graded glycerol solutions. Cartilage tissue was manually dissected out.

Whole-mount *in situ* hybridization (WISH) and sectioning
We used a WISH procedure optimized for NC (Monsoro-Burq, 2007). For sectioning, embryos were embedded in gelatin-albumin and 30-μm-thick vibratome transverse sections were cut.

DEVELOPMENT

Western blotting

Lysates (five to ten whole embryos, 10-15 NBs, NCs or dorsal explants) were prepared using phosphatase (PhosSTOP, Roche) and protease inhibitors (Sigma) and analyzed by standard western blotting (Pegoraro et al., 2015; Table S4).

RT-qPCR

Total RNA was extracted from three to five whole embryos or five NB, NC or dorsal explants (Sive et al., 2010). RT-qPCR was performed according to standard procedures using MIQE recommendations (Pegoraro et al., 2015; Table S3). Results were normalized against the reference genes *odc* (*odc1*) and *ef1a* (*eef1a1*). Primers used to test PFKFB4MO efficiency span the exon1-exon2 region, i.e. include the exon1-intron1 junction targeted by the morpholino.

Statistical analysis, imaging and image processing

All experiments were performed at least three times independently (except experiments shown in Fig. 5A, which were performed in duplicate). The most frequent phenotypes are shown. Graphs indicate the mean percentage of embryos for a given phenotype. NC stream area and NC distance of migration (Fig. 4) were measured using ImageJ software. Error bars represent s.e.m. Student's *t*-test was used to determine statistical significance ($P \leq 0.05$). Images were processed with standard calibration of RGB levels (Photoshop, Gimp).

Supplementary information

Supplementary information available online at
http://dev.biologists.org/lookup/doi/10.1242/dev.157644.supplemental

References

Bahm, I., Barriga, E. H., Frolov, A., Theveneau, E., Frankel, P. and Mayor, R. (2017). PDGF controls contact inhibition of locomotion by regulating N-cadherin during neural crest migration. *Development* **144**, 2456-2468.

Bailey, A. P., Bhattacharyya, S., Bronner-Fraser, M. and Streit, A. (2006). Lens specification is the ground state of all sensory placodes, from which FGF promotes olfactory identity. *Dev. Cell* **11**, 505-517.

Basch, M. L., Bronner-Fraser, M. and García-Castro, M. I. (2006). Specification of the neural crest occurs during gastrulation and requires Pax7. *Nature* **441**, 218-222.

Bellmeyer, A., Krase, J., Lindgren, J. and LaBonne, C. (2003). The protooncogene c-Myc is an essential regulator of neural crest formation in Xenopus. *Dev. Cell* **4**, 827-839.

Betancur, P., Bronner-Fraser, M. and Sauka-Spengler, T. (2010). Assembling neural crest regulatory circuits into a gene regulatory network. *Annu. Rev. Cell Dev. Biol.* **26**, 581-603.

Blum, M., De Robertis, E. M., Wallingford, J. B. and Niehrs, C. (2015). Morpholinos: antisense and sensibility. *Dev. Cell* **35**, 145-149.

Brewer, S., Feng, W., Huang, J., Sullivan, S. and Williams, T. (2004). Wnt1-Cre-mediated deletion of AP-2alpha causes multiple neural crest-related defects. *Dev. Biol.* **267**, 135-152.

Bronner, M. E. and Le Douarin, N. M. (2012). Development and evolution of the neural crest: an overview. *Dev. Biol.* **366**, 2-9.

Chang, C. and Hemmati-Brivanlou, A. (1998). Neural crest induction by Xwnt7B in Xenopus. *Dev. Biol.* **194**, 129-134.

Courtnay, R., Ngo, D. C., Malik, N., Ververis, K., Tortorella, S. M. and Karagiannis, T. C. (2015). Cancer metabolism and the Warburg effect: the role of HIF-1 and PI3K. *Mol. Biol. Rep.* **42**, 841-851.

de Crozé, N., Maczkowiak, F. and Monsoro-Burq, A. H. (2011). Reiterative AP2a activity controls sequential steps in the neural crest gene regulatory network. *Proc. Natl. Acad. Sci. USA* **108**, 155-160.

Essex, L. J., Mayor, R. and Sargent, M. G. (1993). Expression of Xenopus snail in mesoderm and prospective neural fold ectoderm. *Dev. Dyn.* **198**, 108-122.

Fu, Q.-F., Liu, Y., Fan, Y., Hua, S.-N., Qu, H.-Y., Dong, S.-W., Li, R.-L., Zhao, M.-Y., Zhen, Y., Yu, X.-L. et al. (2015). Alpha-enolase promotes cell glycolysis, growth, migration, and invasion in non-small cell lung cancer through FAK-mediated PI3K/AKT pathway. *J. Hemat. Oncol.* **8**, 22.

Han, T., Kang, D., Ji, D., Wang, X., Zhan, W., Fu, M., Xin, H.-B. and Wang, J.-B. (2013). How does cancer cell metabolism affect tumor migration and invasion? *Cell Adh. Migr.* **7**, 395-403.

Heike, C. L., Luquetti, D. V. and Hing, A. V. (1993). Craniofacial microsomia overview. *GeneReviews* (ed. M. P. Adam, H. H. Ardinger, R. A. Pagon, S. E. Wallace, L. J. H. Bean, H. C. Mefford, K. Stephens, A. Amemiya, N. Ledbetter). University of Washington, Seattle, WA, USA.

Ito, K. and Suda, T. (2014). Metabolic requirements for the maintenance of self-renewing stem cells. *Nat. Rev. Mol. Cell Biol.* **15**, 243-256.

Khadka, D., Luo, T. and Sargent, T. D. (2006). Msx1 and Msx2 have shared essential functions in neural crest but may be dispensable in epidermis and axis formation in Xenopus. *Int. J. Dev. Biol.* **50**, 499-502.

LaBonne, C. and Bronner-Fraser, M. (1998). Neural crest induction in Xenopus: evidence for a two-signal model. *Development* **125**, 2403-2414.

Lander, R., Nasr, T., Ochoa, S. D., Nordin, K., Prasad, M. S. and Labonne, C. (2013). Interactions between Twist and other core epithelial-mesenchymal transition factors are controlled by GSK3-mediated phosphorylation. *Nat. Commun.* **4**, 1542.

Le Douarin, N. L. and Kalcheim, C. (1999). *The Neural Crest*. Cambridge, UK: Cambridge University Press.

Li, B., Kuriyama, S., Moreno, M. and Mayor, R. (2009). The posteriorizing gene Gbx2 is a direct target of Wnt signalling and the earliest factor in neural crest induction. *Development* **136**, 3267-3278.

Luo, T., Lee, Y.-H., Saint-Jeannet, J.-P. and Sargent, T. D. (2003). Induction of neural crest in Xenopus by transcription factor AP2alpha. *Proc. Natl. Acad. Sci. USA* **100**, 532-537.

Lwigale, P. Y. (2015). Corneal development: different cells from a common progenitor. *Prog. Mol. Biol. Transl. Sci.* **134**, 43-59.

Maczkowiak, F., Matéos, S., Wang, E., Roche, D., Harland, R. and Monsoro-Burq, A. H. (2010). The Pax3 and Pax7 paralogs cooperate in neural and neural crest patterning using distinct molecular mechanisms, in Xenopus laevis embryos. *Dev. Biol.* **340**, 381-396.

Mancilla, A. and Mayor, R. (1996). Neural crest formation in Xenopus laevis: mechanisms of Xslug induction. *Dev. Biol.* **177**, 580-589.

Mayor, R., Morgan, R. and Sargent, M. G. (1995). Induction of the prospective neural crest of Xenopus. *Development* **121**, 767-777.

Meulemans, D. and Bronner-Fraser, M. (2004). Gene-regulatory interactions in neural crest evolution and development. *Dev. Cell* **7**, 291-299.

Milet, C. and Monsoro-Burq, A. H. (2012). Neural crest induction at the neural plate border in vertebrates. *Dev. Biol.* **366**, 22-33.

Milet, C. and Monsoro-Burq, A. H. (2014). Dissection of Xenopus laevis neural crest for in vitro explant culture or in vivo transplantation. *J. Vis. Exp.* **85**, e51118.

Monsoro-Burq, A. H. (2007). A rapid protocol for whole-mount in situ hybridization on Xenopus embryos. *CSH Protoc.* pdb.prot4809.

Monsoro-Burq, A.-H., Fletcher, R. B. and Harland, R. (2003). Neural crest induction by paraxial mesoderm in Xenopus embryos requires FGF signals. *Development* **130**, 3111-3124.

Monsoro-Burq, A.-H., Wang, E. and Harland, R. (2005). Msx1 and Pax3 cooperate to mediate FGF8 and WNT signals during Xenopus neural crest induction. *Dev. Cell* **8**, 167-178.

Moody, S. A. (1987). Fates of the blastomeres of the 16-cell stage Xenopus embryo. *Dev. Biol.* **119**, 560-578.

Neave, B., Holder, N. and Patient, R. (1997). A graded response to BMP-4 spatially coordinates patterning of the mesoderm and ectoderm in the zebrafish. *Mech. Dev.* **62**, 183-195.

DEVELOPMENT

Nichane, M., de Crozé, N., Ren, X., Souopgui, J., Monsoro-Burq, A. H. and Bellefroid, E. J. (2008). Hairy2-Id3 interactions play an essential role in Xenopus neural crest progenitor specification. *Dev. Biol.* **322**, 355-367.

Nieto, M. A., Sargent, M. G., Wilkinson, D. G. and Cooke, J. (1994). Control of cell behavior during vertebrate development by Slug, a zinc finger gene. *Science* **264**, 835-839.

Nieuwkoop, P. D. and Faber, J. (1994). *Normal Table of Xenopus Laevis (Daudin): A Systematical and Chronological Survey of the Development from the Fertilized Egg Till the End of Metamorphosis*. New York, USA: Garland Pub.

Okar, D. A., Manzano, A., Navarro-Sabatè, A., Riera, L., Bartrons, R. and Lange, A. J. (2001). PFK-2/FBPase-2: maker and breaker of the essential biofactor fructose-2, 6-bisphosphate. *Trends Biochem. Sci.* **26**, 30-35.

Pegoraro, C. and Monsoro-Burq, A. H. (2012). Signaling and transcriptional regulation in neural crest specification and migration: lessons from xenopus embryos. *Dev. Biol.* **2**, 247-259.

Pegoraro, C., Figueiredo, A. L., Maczkowiak, F., Pouponnot, C., Eychène, A. and Monsoro-Burq, A. H. (2015). PFKFB4 controls embryonic patterning via Akt signalling independently of glycolysis. *Nat. Commun.* **6**, 5953.

Pilkis, S. J., Claus, T. H. and Kurland, I. J. (1995). 6-Phoshphofructo-2-kinase/ Fructose-2,6-bisphosphatase: a metabolic signaling enzyme. *Annu. Rev. Biochem.* **64**, 799-835.

Plouhinec, J.-L., Roche, D. D., Pegoraro, C., Figueiredo, A. L., Maczkowiak, F., Brunet, L. J., Milet, C., Vert, J.-P., Pollet, N., Harland, R. M. et al. (2014). Pax3 and Zic1 trigger the early neural crest gene regulatory network by the direct activation of multiple key neural crest specifiers. *Dev. Biol.* **386**, 461-472.

Qu, J., Lu, D., Guo, H., Miao, W., Wu, G. and Zhou, M. (2016). PFKFB3 modulates glycolytic metabolism and alleviates endoplasmic reticulum stress in human osteoarthritis cartilage. *Clin. Exp. Pharmacol. Physiol.* **43**, 312-318.

Saint-Jeannet, J. P., Foulquier, F., Goridis, C. and Duprat, A. M. (1989). Expression of N-CAM precedes neural induction in Pleurodeles waltl (urodele, amphibian). *Development* **106**, 675-683.

Saint-Jeannet, J.-P., He, X., Varmus, H. E. and Dawid, I. B. (1997). Regulation of dorsal fate in the neuraxis by Wnt-1 and Wnt-3a. *Proc. Natl. Acad. Sci. USA* **94**, 13713-13718.

Sato, T., Sasai, N. and Sasai, Y. (2005). Neural crest determination by co-activation of Pax3 and Zic1 genes in Xenopus ectoderm. *Development* **132**, 2355-2363.

Simões-Costa, M., Stone, M. and Bronner, M. E. (2015). Axud1 integrates Wnt signaling and transcriptional inputs to drive neural crest formation. *Dev. Cell* **34**, 544-554.

Sive, H. L., Grainger, R. M. and Harland, R. M. (2010). *Early Development of Xenopus Laevis: A Laboratory Manual*. Cold Spring Harbor, NY, USA: Cold Spring Harbor Laboratory Press.

Steventon, B., Araya, C., Linker, C., Kuriyama, S. and Mayor, R. (2009). Differential requirements of BMP and Wnt signalling during gastrulation and neurulation define two steps in neural crest induction. *Development* **136**, 771-779.

Theveneau, E. and Mayor, R. (2012). Neural crest delamination and migration: from epithelium-to-mesenchyme transition to collective cell migration. *Dev. Biol.* **366**, 34-54.

Théveneau, E., Duband, J.-L. and Altabef, M. (2007). Ets-1 confers cranial features on neural crest delamination. *PLoS ONE* **2**, e1142.

Trefely, S., Khoo, P.-S., Krycer, J. R., Chaudhuri, R., Fazakerley, D. J., Parker, B. L., Sultani, G., Lee, J., Stephan, J.-P., Torres, E. et al. (2015). Kinome screen identifies PFKFB3 and glucose metabolism as important regulators of the Insulin/ Insulin-like Growth Factor (IGF)-1 signaling pathway. *J. Biol. Chem.* **290**, 25834-25846.

Vega, S., Morales, A. V., Ocaña, O. H., Valdés, F., Fabregat, I. and Nieto, M. A. (2004). Snail blocks the cell cycle and confers resistance to cell death. *Genes Dev.* **18**, 1131-1143.

Villanueva, S., Glavic, A., Ruiz, P. and Mayor, R. (2002). Posteriorization by FGF, Wnt, and retinoic acid is required for neural crest induction. *Dev. Biol.* **241**, 289-301.

Wilson, P. A., Lagna, G., Suzuki, A. and Hemmati-Brivanlou, A. (1997). Concentration-dependent patterning of the Xenopus ectoderm by BMP4 and its signal transducer Smad1. *Development* **124**, 3177-3184.

Wilson, N. R., Olm-Shipman, A. J., Acevedo, D. S., Palaniyandi, K., Hall, E. G., Kosa, E., Stumpff, K. M., Smith, G. J., Pitstick, L., Liao, E. C. et al. (2016). SPECC1L deficiency results in increased adherens junction stability and reduced cranial neural crest cell delamination. *Sci. Rep.* **6**, 17735.

DEVELOPMENT